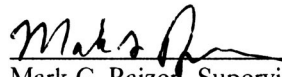


Copyright
by
Daniel Adam Steck
2001

The Dissertation Committee of Daniel Adam Steck certifies that this
is the approved version of the following dissertation:

**QUANTUM CHAOS, TRANSPORT, AND DECOHERENCE IN ATOM
OPTICS**

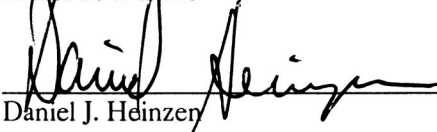
Committee:



Mark G. Raizen, Supervisor



Rafael de la Llave



Daniel J. Heinzen



Philip J. Morrison



Qian Niu

**QUANTUM CHAOS, TRANSPORT, AND DECOHERENCE IN ATOM
OPTICS**

by

DANIEL ADAM STECK, B.S.

DISSERTATION

Presented to the Faculty of the Graduate School of

The University of Texas at Austin

in Partial Fulfillment

of the Requirements

for the Degree of

DOCTOR OF PHILOSOPHY

THE UNIVERSITY OF TEXAS AT AUSTIN

December 2001

Acknowledgements

Experimental research is often a collaborative endeavor, and the work presented in this dissertation is certainly no exception. During the past six years I have had the pleasure of working with a number of bright and enthusiastic people that I would like to mention here.

First of all, I would like to thank my advisor, Mark Raizen. Mark is always brimming with intriguing new ideas, and he has an exceptional sense for interesting physics problems. Mark has provided an exciting and supportive research environment for his students. I have truly enjoyed and greatly benefited from spending the past few years under his guidance.

I have collaborated with Windell Oskay on all of the research in this dissertation. I cannot imagine having done the experiments in this dissertation without Windell's remarkable productivity and superior technical prowess. This is especially true of the chaos-assisted tunneling experiments in Chapter 6, where the two of us managed an enormously complicated experiment and took enough data to literally choke our computer. Windell's rock-solid and extensive LabVIEW code (which featured its own web page so that we could check on the status of the experiment from anywhere in the world) enabled the 12 and 33 day (running 24/7) data marathons that produced all of the CAT results. It was also great to work with someone that shares my ardor for doing things the "right" way, and I have appreciated his attention to detail. I should also note that Windell is responsible for nearly all of the 3D renderings in this dissertation, including the nice surface plots of the data in Chapter 6. It has been a pleasure knowing Windell both in and out of the lab, who has excellent taste in movies, art, italian cuisine, chocolate, and computers.

I worked with Bruce Klappauf from nearly the beginning of my graduate studies to build up the cesium experiment from scratch, and he worked on the early kicked-rotor experiments in Chapter 4. Bruce is not only laid back and very easy to work with, but also good at simply making

things work. His insight, creativity, and curiosity made him a great asset to the lab as well as a great guy to hang out with.

Our postdoc Valery Milner also worked on the later kicked-rotor experiments on quantum–classical correspondence in Chapter 4. It seemed that every time he touched the Ti:sapphire laser, he would set a new record for its output power. His deftness in handling the laser was a crucial factor in enabling these experiments. Valery is also an imaginative and intelligent problem solver, and I have enjoyed many physics discussions with him.

I would also like to acknowledge the other students working on the cesium experiment. Alex Mück and Nicole Helbig, two Würzburg students, took on challenging projects to implement a new measurement technique and a high-intensity laser source, while at the same time providing colorful company. The cesium experiment will be in good hands with the next generation of students, Jay Hanssen, Todd Meyrath, and Chuanwei Zhang, whatever the experiment becomes in the future. Special thanks to Jay and Todd for helping to babysit the experiment during the final “datathon.”

I also enjoyed interacting with people over on the sodium side of the lab. Cyrus Bharucha has been a great friend and roommate in addition to being a talented physicist in the laboratory, continually posing interesting puzzles and questions, always with a cheerful demeanor. I have profited immensely from many memorable and long discussions with Kirk Madison, whose peculiar sense of humor and fervor for physics (and many other things) have made him a terrific colleague and friend. Martin Fischer is an exceptionally skilled experimentalist, with a broad knowledge of physics and a singular ability to explain things clearly. His advice, insight, and presence in the lab contributed much to my development as a scientist.

Thanks also go to Pat Morrow, who provided good advice and a lot of great experimental knowledge when I first arrived, as well as help in getting the Ti:sapphire laser to flash. Postdoc Steve Wilkinson brought a great deal of experience to the lab and was also a great source of knowledge when I was starting out. Many other members of the Raizen Lab made it a great place

to be, even though I didn't get to work directly with them: John Robinson, Braulio Gutiérrez-Medina, Artëm Dudarev, Kevin Henderson (whose digital camera I used to take the photographs in this dissertation), Artur Widera, Patrick Bloom, Greg Henry, Arnaud Cursente, Wes Campbell, and Fred the mouse. Thanks also to Adrienne Lipoma and Julie Horn for keeping the lab running smoothly.

I have learned much during my graduate studies, due in no small part to the presence of many top-notch researchers at UT. In particular, I would like to mention Bala Sundaram, who is a truly brilliant guy and has been a great source of knowledge about classical and quantum chaos; Matt Choptuik, whose skill and willingness to help were invaluable in enabling my high-performance computing efforts; and Phil Morrison, from whom I learned a tremendous amount about classical Hamiltonian dynamics.

The Physics Department staff at UT was also of inestimable help. Les Deavers and later Allan Schroeder ran a group of top-notch machinists, whose services were indispensable during the construction phases of the experiment. I would also like to thank the administrative staff, especially Norma Kotz, Glenn Suchan, Dorothy Walker, and Olga Vorloou, for all their assistance.

Of course, I could not have come this far without a good start in physics, and the University of Dayton was an ideal place to be an undergraduate. I am grateful to have had such a great group of faculty and fellow students to nurture my yearning to study physics. Special thanks to Perry Yaney, who gave me my first taste of research, and who was a great mentor in so many ways. I would also like to thank Leno Pedrotti, from whom I garnered a love of things quantum; John Erdei, who piqued my interest in chaotic systems (and from whom I learned of the demonstration in Fig. 1.1); Bob Brecha, who alerted me to the fact that there were really great things going on in Mark's lab here at UT; and Mike O'Hare, for running a great department. The experience and knowledge gained in my undergraduate research under Brian Kennedy was also of much value in my later research. Thanks also to Alba Hurlbut, my high school physics teacher, for encouraging me to go into physics.

I would like to thank Windell Oskay, Patrick Bloom, Kirk Madison, Rafael de la Llave, Phil Morrison, Daniel Heinzen, Martin Fischer, Jay Hanssen, and Todd Meyrath for valuable comments and corrections. This dissertation has also benefited from discussions with Simon Gardiner, Salman Habib, Kurt Jacobs, Amaury Mouchet, and Vitali Averbukh.

I would also like to acknowledge financial support from a National Science Foundation Graduate Research Fellowship during the first three years and a Fannie and John Hertz Foundation Fellowship during the final three years of my graduate studies. The research effort as a whole was supported by the National Science Foundation, the Robert A. Welch Foundation, the Sid W. Richardson Foundation, and the U.S.–Israeli Binational Science Foundation. I performed some of the computations in this dissertation on supercomputers at the Texas Advanced Computing Center.

Finally, I would like to thank my parents, Raymond and Shitsuko Steck, for encouraging me to follow my interests and fostering in me a curiosity for how things work.

D. A. S.
Austin, Texas
October, 2001

QUANTUM CHAOS, TRANSPORT, AND DECOHERENCE IN ATOM OPTICS

Publication No. _____

Daniel Adam Steck, Ph.D.
The University of Texas at Austin, 2001

Supervisor: Mark G. Raizen

This dissertation details an experimental investigation of the center-of-mass motion of cesium atoms in a time-dependent lattice of light. The research described here proceeds along two general lines. The first group of experiments considers a realization of the quantum kicked rotor, where the optical lattice is applied in a series of short, periodic pulses. In the regime where the classical description of this system is strongly chaotic, the quantum and classical dynamics differ remarkably due to dynamical localization, which is a manifestation of the quantum suppression of classical chaos. Because this quantum localization is a coherent effect, it should be vulnerable to noise or coupling to the environment, providing a mechanism for restoring classical behavior at the macroscopic level. The experimental results confirm that dynamical localization can be destroyed by adding noise and dissipation in a controlled way, and furthermore they show that quantitative agreement between the experiment and a classical model can be reached with a sufficient level of applied noise.

The second line of research considers the weakly chaotic regime, where stable and chaotic regions coexist in phase space. The optical lattice is modulated sinusoidally in these experiments to realize the amplitude-modulated pendulum. Careful preparation of the initial atomic state, including stimulated Raman velocity selection, is necessary to resolve the phase-space features. Coherent tunneling oscillations are observed between two symmetry-related

islands of stability in phase space. Because the classical transport between the islands is forbidden by the system dynamics, as opposed to a potential barrier, the tunneling in this experiment is an example of dynamical tunneling. Additionally, the experimental data indicate through multiple signatures that the tunneling is enhanced by the presence of the chaotic region in phase space, an effect known as chaos-assisted tunneling.

Table of Contents

Acknowledgements	vii
Abstract	xi
List of Tables	xix
List of Figures	xxi
Chapter 1. Introduction	1
1.1 Classical Chaos	2
1.1.1 Phase Space	7
1.1.2 Integrability and Chaos	11
1.2 Quantum Chaos	14
1.2.1 Quantum Chaology	16
1.2.2 Chaos in Quantum Mechanics	18
1.2.3 Experiments in Quantum Chaos	20
1.2.4 On the “Usefulness” of Quantum Chaos	21
1.3 Decoherence	22
1.3.1 Suppression of Quantum Superposition	24
1.3.2 Classical Chaotic Evolution	27
1.3.3 Experiments on Decoherence	31
1.4 Atom Optics	32
1.4.1 The Dipole Force and Optical Lattices	34
1.4.2 Atom Optics and Quantum Chaos	35
Chapter 2. Atomic Motion in an Optical Standing Wave	39
2.1 Overview	40
2.2 Atom-Field Interaction	41
2.2.1 Digression: Unitary Transformations and Field Operators	43
2.3 Schrödinger Equation	45

2.4	Adiabatic Approximation	46
2.4.1	Master Equation Approach	47
2.5	Complications	50
2.5.1	Spontaneous Emission	50
2.5.2	Stochastic Dipole Force	51
2.5.3	Nonlinearities of the Potential	51
2.5.4	Velocity Dependence	52
2.5.5	Multilevel Structure of Cesium	53
2.5.6	Collisions	54
2.5.7	Experimental Values	54
2.6	Generalization to Two Nonidentical Traveling Waves	56
2.7	Quantum Dynamics in a Stationary Standing Wave	57
2.7.1	Bragg Scattering	58
2.7.2	Band Structure	62
2.7.3	Boundary Conditions	65
Chapter 3. Experimental Apparatus I		67
3.1	Overview	68
3.2	DBR Laser	68
3.2.1	Construction and Operation	69
3.2.2	Saturated Absorption Spectroscopy	71
3.3	Grating-Stabilized Diode Laser	75
3.3.1	Construction and Operation	75
3.3.2	Frequency Control	79
3.4	Ti:sapphire Laser	81
3.4.1	Laser Design and Construction	82
3.4.2	Laser Operation and Control	83
3.4.3	Intensity Calibration	87
3.5	Vacuum System	89
3.5.1	Magnetic Field Control	92
3.6	Imaging System	93
3.7	Measurement Technique	94
3.8	Control Electronics	98

Chapter 4. Localization and Decoherence in the Kicked Rotor	101
4.1 Overview	102
4.2 Rescaling	102
4.3 Standard Map	104
4.4 Classical Transport	106
4.4.1 Diffusion and Correlations	106
4.4.2 Accelerator Modes	109
4.4.3 External Noise	111
4.4.4 Finite-Pulse Effects	114
4.5 Quantum Transport	116
4.5.1 Quantum Mapping	117
4.5.2 Dynamical Localization	119
4.5.3 Quantum Resonances	121
4.5.4 Delocalization	124
4.5.5 Quantum Correlations	127
4.6 Quantitative Study of Delocalization	131
4.6.1 Classical Model of the Experiment	131
4.6.2 Data and Results	138
4.6.2.1 Detailed Study: Destruction of Exponential Localization	141
4.6.2.2 Detailed Study: Regime of Classical Anomalous Diffusion	145
4.7 Comparison with a Universal Theory of Quantum Transport	149
4.8 Calculation of the Correlations	153
4.8.1 Classical Correlations	153
4.8.2 Quantum Correlations	156
Chapter 5. Experimental Apparatus II	159
5.1 Overview	160
5.2 Cooling in a Three-Dimensional Optical Lattice	160
5.3 Stimulated Raman Velocity Selection	165
5.3.1 Stimulated Raman Transitions: General Theory	165
5.3.2 Pulse-Shape Considerations	171
5.3.3 Implementation of Stimulated Raman Transitions	175
5.3.4 Optical Pushing and Hyperfine State Detection	179

5.3.5	Hyperfine Magnetic Sublevel Optical Pumping	181
5.3.6	Implementation of Stimulated Raman Velocity Selection	184
5.3.7	Raman Cooling	185
5.4	Interaction-Potential Phase Control	186
5.5	State-Preparation Sequence	189
5.6	Calibration of the Optical Potential	192
5.6.1	Anharmonicity	193
5.6.2	Quantum Effective Potentials	193
5.6.2.1	Wigner-Function Derivation	195
5.6.3	Calibration by Simulation	197
Chapter 6. Chaos-Assisted Tunneling		199
6.1	Overview	200
6.2	Barrier Tunneling	200
6.3	Dynamical Tunneling	204
6.3.1	Tunneling in Atom Optics	206
6.3.2	Broken Symmetry	211
6.3.3	Tunneling Dependence on Wave-Packet Location	216
6.4	Chaos-Assisted Tunneling	218
6.4.1	Singlet-Doublet Crossings	220
6.4.2	Comparison with Integrable Tunneling	222
6.4.3	Tunneling Dependence on Parameter Variations	226
6.4.4	Floquet Spectra	232
6.4.5	High Temporal Resolution Measurements	236
6.4.6	Transport in the Strongly Coupled Regime	241
6.5	Noise Effects on Tunneling	243
6.5.1	Chebyshev Filter Response	246
Appendices		249

Appendix A. Cesium D Line Data	251
A.1 Overview	251
A.2 Cesium Physical and Optical Properties	251
A.3 Hyperfine Structure	253
A.3.1 Energy Level Splittings	253
A.3.2 Interaction with Static External Fields	255
A.3.2.1 Magnetic Fields	255
A.3.2.2 Electric Fields	257
A.3.3 Reduction of the Dipole Operator	258
A.4 Resonance Fluorescence	260
A.4.1 Symmetries of the Dipole Operator	260
A.4.2 Resonance Fluorescence in a Two-Level Atom	261
A.4.3 Optical Pumping	262
A.4.3.1 Circularly (σ^\pm) Polarized Light	264
A.4.3.2 Linearly (π) Polarized Light	265
A.4.3.3 One-Dimensional $\sigma^+ - \sigma^-$ Optical Molasses	265
A.4.3.4 Three-Dimensional Optical Molasses	265
A.5 Data Tables	268
Appendix B. Phase Space Gallery I: Standard Map	281
Appendix C. Phase Space Gallery II: Amplitude-Modulated Pendulum	291
Bibliography	305
Index	335
Vita	339

List of Tables

2.1	Numerical estimates for deviations from an ideal optical lattice	55
A.1	Fundamental Physical Constants	268
A.2	Cesium Physical Properties	268
A.3	Cesium D ₂ Transition Optical Properties	269
A.4	Cesium D ₁ Transition Optical Properties	269
A.5	Cesium D Transition Hyperfine Structure Constants	269
A.6	Cesium D Transition Magnetic/Electric Field Interaction Parameters	270
A.7	Cesium Dipole Matrix Elements and Saturation Intensities	270
A.8	Cesium Relative Hyperfine Transition Strength Factors $S_{FF'}$	270
A.9	Cesium D ₂ Transition Dipole Matrix Elements	271
A.10	Cesium D ₂ Transition Dipole Matrix Elements	271
A.11	Cesium D ₂ Transition Dipole Matrix Elements	271
A.12	Cesium D ₂ Transition Dipole Matrix Elements	272
A.13	Cesium D ₂ Transition Dipole Matrix Elements	272
A.14	Cesium D ₂ Transition Dipole Matrix Elements	272
A.15	Cesium D ₁ Transition Dipole Matrix Elements	273
A.16	Cesium D ₁ Transition Dipole Matrix Elements	273
A.17	Cesium D ₁ Transition Dipole Matrix Elements	273
A.18	Cesium D ₁ Transition Dipole Matrix Elements	274
A.19	Cesium D ₁ Transition Dipole Matrix Elements	274
A.20	Cesium D ₁ Transition Dipole Matrix Elements	274

List of Figures

1.1	Numerical instability in the standard map	6
1.2	Pendulum phase space	8
1.3	Weakly driven pendulum phase space	10
1.4	Strongly driven pendulum phase space	11
1.5	Numerical time-reversal of the classical and quantum kicked rotor	17
2.1	Level diagram for second-order Bragg scattering	59
2.2	Band structure of an optical standing wave potential	62
2.3	Dependence of allowed energies on the quasimomentum	63
3.1	DBR laser collimating lens mount assembly	71
3.2	Photograph of DBR laser system	72
3.3	Optical table layout	73
3.4	DBR laser saturated-absorption spectrum	74
3.5	Grating-stabilized laser diode assembly	77
3.6	Photograph of the grating-stabilized laser system	78
3.7	Repump laser saturated absorption spectrum (photodiode output)	80
3.8	Repump laser saturated absorption spectrum (lock-in output)	81
3.9	Ti:sapphire laser schematic layout	84
3.10	Ti:sapphire laser photograph (overall view)	85
3.11	Ti:sapphire laser photograph (cavity detail)	86
3.12	Vacuum chamber photograph (overall)	89
3.13	Vacuum chamber photograph (main section)	90
3.14	Schematic of experimental sequence	95
3.15	Measured momentum distribution of MOT atoms	97
4.1	Diffusion rate vs. K in the standard map	108
4.2	Standard-map trajectories with and without Lévy flights	110
4.3	Diffusion rate plot for various amplitude noise levels	114

4.4	Phase space comparison between δ -kicks and square pulses	115
4.5	Experimental momentum evolution with dynamical localization	121
4.6	Experimental measurement of dynamical localization (log plot)	122
4.7	Quantum resonances in experiment and simulation	123
4.8	Enhanced energy growth due to delocalization by optical molasses	125
4.9	Optical molasses effects on quantum kicked rotor evolution	126
4.10	Experimental verification of the Shepelyansky scaling for K_q	129
4.11	Influence of accelerator modes on momentum distributions	130
4.12	Systematic effects in the experiment on measured energies	132
4.13	Experimental laser pulse for kicked-rotor realization	134
4.14	Amplitude noise effects on energy vs. K curves	139
4.15	Experimental and classical ensemble energies with noise, $K = 11.2$	142
4.16	Experimental and classical ensemble energy evolution, $K = 11.2$	143
4.17	Experimental and classical momentum distributions, $K = 11.2$	144
4.18	Experimental and classical ensemble energies with noise, $K = 8.4$	146
4.19	Experimental and classical ensemble energy evolution, $K = 8.4$	147
4.20	Experimental and classical momentum distributions, $K = 8.4$	148
4.21	Quantum diffusion theory fit to a localized case	150
4.22	Quantum diffusion theory fit to a noise-driven case	151
4.23	Quantum diffusion theory fit to an anomalous transport case	152
5.1	Diagram of three-dimensional lattice geometry	161
5.2	Stimulated Raman transition energy levels	166
5.3	Spectral excitation profile due to a square Raman pulse	172
5.4	Time evolution of Raman-excited population	173
5.5	Comparison of square and Blackman pulse excitation profiles	174
5.6	Stimulated Raman implementation optical layout	175
5.7	Energy-level scheme for reversible stimulated Raman tagging	176
5.8	Optical layout of pumping and pushing beams for Raman tagging	179
5.9	Experimental Raman Rabi oscillations in copropagating mode	181
5.10	Experimental Raman Rabi oscillations in counterpropagating mode	182
5.11	Experimental Raman-transition profiles in copropagating mode	183
5.12	Photograph of optical lattice phase-control setup	187

5.13	Electro-optic modulator response to a sudden phase change	188
5.14	Schematic picture of state-preparation sequence	190
5.15	Comparison of classical and quantum pendulum motion	194
5.16	Experimentally measured pendulum oscillation periods	197
6.1	Tunneling doublet in the quartic double well potential	201
6.2	Two-level avoided crossing	203
6.3	Phase space for the quartic double-well potential	204
6.4	Experimental initial condition in phase space	209
6.5	Observation of coherent tunneling oscillations	210
6.6	Detail of momentum distributions showing tunneling oscillations	210
6.7	Influence of Raman-pulse duration on tunneling	212
6.8	Tunneling measurement without Raman velocity selection	213
6.9	Influence of Raman-pulse detuning on tunneling	214
6.10	Simulation of Raman tag width effects on tunneling	215
6.11	Influence of spatial displacement of the initial condition on tunneling	216
6.12	Displaced initial conditions for various time delays	217
6.13	Three-level avoided crossing	221
6.14	Corresponding pendulum phase space	223
6.15	Comparison of modulated-pendulum tunneling to Bragg scattering	224
6.16	Modulated-pendulum tunneling for $\hbar k = 1.04$	225
6.17	Tunneling variation vs. α , for $\hbar k = 2.08$	227
6.18	Tunneling rate vs. α , for $\hbar k = 2.08$	228
6.19	Tunneling for $\alpha = 8.0$, for $\hbar k = 2.08$	229
6.20	Tunneling for $\alpha = 9.7$, for $\hbar k = 2.08$	229
6.21	Tunneling variation vs. α , for $\hbar k = 1.04$	230
6.22	Tunneling rate vs. α , for $\hbar k = 1.04$	231
6.23	Calculated Floquet spectrum for $\hbar k = 2.077$	234
6.24	Calculated Floquet spectrum for $\hbar k = 1.039$	235
6.25	Fine time step evolution, $\hbar k = 2.08, \alpha = 7.7$	236
6.26	Fine time step evolution, $\hbar k = 2.08, \alpha = 11.2$	237
6.27	Fine time step evolution, $\hbar k = 1.04, \alpha = 10.5$	238
6.28	Evolution of classical phase space at different sampling phases	239

6.29	Strongly coupled transport, $\hbar k = 2.08$, $\alpha = 17.0$	241
6.30	Strongly coupled transport, $\hbar k = 2.08$, $\alpha = 18.9$	242
6.31	Illustration of amplitude noise applied to the optical lattice intensity	243
6.32	Effects of amplitude noise on tunneling, $\hbar k = 2.08$	244
6.33	Effects of amplitude noise on tunneling, $\hbar k = 1.04$	245
6.34	Chebyshev filter frequency response	247
A.1	Dependence of cesium vapor pressure on temperature	275
A.2	Cesium D_2 transition hyperfine structure	276
A.3	Cesium D_1 transition hyperfine structure	277
A.4	Cesium $6^2S_{1/2}$ level hyperfine structure in an external magnetic field	278
A.5	Cesium $6^2P_{1/2}$ level hyperfine structure in an external magnetic field	278
A.6	Cesium $6^2P_{3/2}$ level hyperfine structure in an external magnetic field	279
A.7	Cesium $6^2P_{3/2}$ level hyperfine structure in an external electric field	279